

## RESEARCH ARTICLE

WILEY

# Characterizing seasonal groundwater storage in alpine catchments using time-lapse gravimetry, water stable isotopes and water balance methods

Marie Arnoux  | Landon J. S. Halloran | Eléonore Berdat | Daniel Hunkeler

Centre d'Hydrogéologie et de Géothermie (CHYN), Université de Neuchâtel, Neuchâtel, Switzerland

## Correspondence

Marie Arnoux, Centre d'Hydrogéologie et de Géothermie (CHYN), Université de Neuchâtel, Rue Emile Argand 11, 2000 Neuchâtel, Switzerland.  
Email: marie.arnoux@protonmail.com

## Abstract

Alpine areas play a major role in water supply in downstream valleys by releasing water during warm and dry periods. However, the hydrogeology of alpine catchments, which are particularly exposed to the effects of climate change, is currently not well understood. Increasing our knowledge of alpine hydrogeological processes is thus of considerable importance for any forward-looking hydrological investigations in alpine areas. The objectives of this study are to quantify seasonal groundwater storage variations in a small Swiss alpine catchment and to evaluate the capabilities of time-lapse gravimetry in the identification of zones of high groundwater storage fluctuations. Time-lapse gravimetric measurements enable rapid localisation of zones of dynamic groundwater storage changes and help to highlight aquifers with a higher storage decrease. Temperature sensors enable measurement of the temporal trend in stream and spring drying in the post-snowmelt period. Stable isotope measurements allow us to identify the origin of surface water exiting the catchment. The results improve our comprehension of a conceptual schema highlighting two different hydrogeological systems: (a) a shallow, rapidly depleted one fed directly by snowmelt and (b) a deeper one, with a slower recession, fed by main recharge during peak snowmelt and emerging at the lower part of the catchment below the talus and moraine of the catchment where bedrock is exposed. These dynamics confirm the high variability of storage in the talus and moraine aquifers and highlight the dominant role of Quaternary deposits and their connectivity to store water over seasonal and multi-year time-scales. The mechanisms explaining the importance of Quaternary deposits are the combination of moraine and talus with different permeabilities allowing the storage of sufficient quantities of water permitting continuous release during drier periods of the year.

## KEYWORDS

alpine catchment, gravimetry, groundwater storage, stable isotopes, surface water-groundwater interactions

## 1 | INTRODUCTION

Alpine regions sustain water resources in downstream valleys by releasing meltwater during warm and dry periods. Alpine areas are steep

mountainous regions that are located mostly above the tree line and are snowmelt dominated. Their seasonal redistribution of water can act as a buffer to significantly reduce the implications of meteorological droughts in lowlands during summer (Beniston & Stoffel, 2014; Rohrer,

Salzmann, Stoffel, & Kulkarni, 2013). However, the reduction of snow cover periods in a warming climate threatens the sustainability of these important reservoirs (Barnett, Adam, & Lettenmaier, 2005; Immerzeel et al., 2020; Viviroli, Dürr, Messerli, Meybeck, & Weingartner, 2007).

Hydrogeological processes, that is, hydrological processes pertaining to the subsurface, can play an important role in buffering climate change impacts in these areas (Hayashi, 2020). In research of these regions, groundwater has frequently been ignored (Huss, Farinotti, Bauder, & Funk, 2008; Juen, Kaser, & Georges, 2007), although its often significant contribution to alpine streamflow, especially during winter low flows, is now commonly accepted (Clow et al., 2003; Cras, Marc, & Travi, 2007; Hood, Roy, & Hayashi, 2006; Huth, Leydecker, Sickman, & Bales, 2004; Jodar et al., 2017; Liu, Williams, & Caine, 2004). Because alpine hydrogeological processes are still not well understood, it remains unclear to what extent groundwater stored in alpine catchments ensure continuous water supply to lower elevations, both at the present and in future climate change scenarios (Hayashi, 2020). This lack of knowledge can be attributed to two specificities of alpine areas: (a) the large number of small, interacting aquifers and their high levels of heterogeneity and (b) the inherent difficulties in accessing and monitoring the alpine subsurface in order to obtain reliable hydrogeological data which can be used to study groundwater processes and constrain hydrogeological models.

The recent review of Hayashi (2020) illustrated the importance of Quaternary deposit units (such as talus, moraines, meadows or rock glaciers) to store groundwater in alpine areas, as shown by the previous studies of Roy and Hayashi (2009) and Langston, Bentley, Hayashi, McClymont, and Pidlisecky (2011) for talus and moraines, Glas et al. (2019) for talus and meadows and Pauritsch, Wagner, Winkler, and Birk (2016) for relict rock glaciers. Cochand, Christe, Ornstein, and Hunkeler (2019) proposed a conceptual model highlighting the combination of different unconsolidated aquifer units to store groundwater. The recent study of Christensen, Hayashi, and Bentley (2020) identified that in a talus-moraine feature in the Canadian Rockies, groundwater from the moraine supplies most of the water to the basin outlet springs and that moraine, located downstream the talus, could serve as a “gate keeper” of the basin. While knowledge alpine hydrogeology is advancing with more and more studies, current knowledge remains limited and difficult to extrapolate to other alpine areas (Christensen et al., 2020; Somers et al., 2019). As a result, most studies about alpine areas oversimplify groundwater processes in hydrological models. There is therefore an urgent need to find new methods to obtain reliable hydrogeological information in order to better understand the capacity and dynamics of these areas to store water in aquifers.

As it is generally impractical and difficult to drill boreholes in alpine aquifers such as talus or moraine, non-intrusive methods are often preferred. A wide variety of geophysical methods have been employed to image internal structures and characterize physical properties within talus and moraine deposits. These include ground-penetrating radar (Ardelean, Onaca, Urdea, & Sarasan, 2017), electrical resistivity tomography (McClymont, Hayashi, Bentley, Muir, & Ernst, 2010; McClymont et al., 2011), electromagnetic induction

methods (Bucki, Echelmeyer, & MacInnes, 2004), seismic refraction (Langston et al., 2011), and surface nuclear magnetic resonance (Lehmann-Horn et al., 2011). These methods give essential information on hydrological and geophysical characteristics of alpine aquifers, such as the volume of the deposits, the location of wet and dry areas and the presence of internal structures that may control groundwater flow paths (Clow et al., 2003; McClymont et al., 2011), but do not directly quantify groundwater storage variations. Time-lapse gravimetry is another geophysical technique that can help quantify fluctuations in subsurface water. Because repeated gravity surveys reveal changes in local mass with time, the time-lapse data can provide a measurement of water-content changes. Notably, only relative measurements of gravity, rather than absolute values, are required with this approach. This method has been used in one alpine study in the Canadian Rocky Mountains to quantify groundwater changes between maximum storage at the end of the melt period and before the beginning of the snow cover period (McClymont, Hayashi, Bentley, & Liard, 2012). There, the authors found small gravity changes, on the order of method uncertainties.

Here, we use a suite of methods to characterize changes in groundwater storage in a small, alpine catchment: stream and springs monitoring with water stable isotopic measurements, water balance and time-lapse gravimetry. As water-balance methods only provide catchment-scale values, we test whether an approach including single-day gravity surveys at two different points in time could be a feasible option for identifying hotspots of groundwater storage changes. We combine time-lapse gravimetry with water stable isotope measurements, temperature and flow rate measurements of springs and streams. Such a combination of approaches allows us to characterize, both temporally and spatially, the dynamics of an archetypal alpine catchment during the period between the end of snowmelt and the beginning of snow accumulation, with each method providing complimentary quantitative or qualitative information. The studied sub-catchment, dominated by talus and moraine fields, is known to have important groundwater contribution to the catchment outflow (Cochand et al., 2019). Furthermore, this aquifer complex is located on the upper slope portion of the sub-catchment, where groundwater volume changes between the end of the melt period and the beginning of the snow cover period are expected to be at their most significant. The objectives of this study are therefore to (a) quantify local groundwater storage variations during a period of important changes in an alpine catchment, (b) evaluate the ability of time-lapse gravimetry to identify zones of high groundwater storage fluctuations, (c) improve our comprehension of groundwater storage processes in alpine catchments.

## 2 | STUDY SITE

The Tsalet catchment is a typical small alpine catchment, snowmelt dominated, with a surface of 1 km<sup>2</sup>. It is a sub-catchment of the Vallon de Réchy, located in the southeast part of the Swiss Alps (Valais -Figure 1). The Tsalet catchment has an altitude ranging from

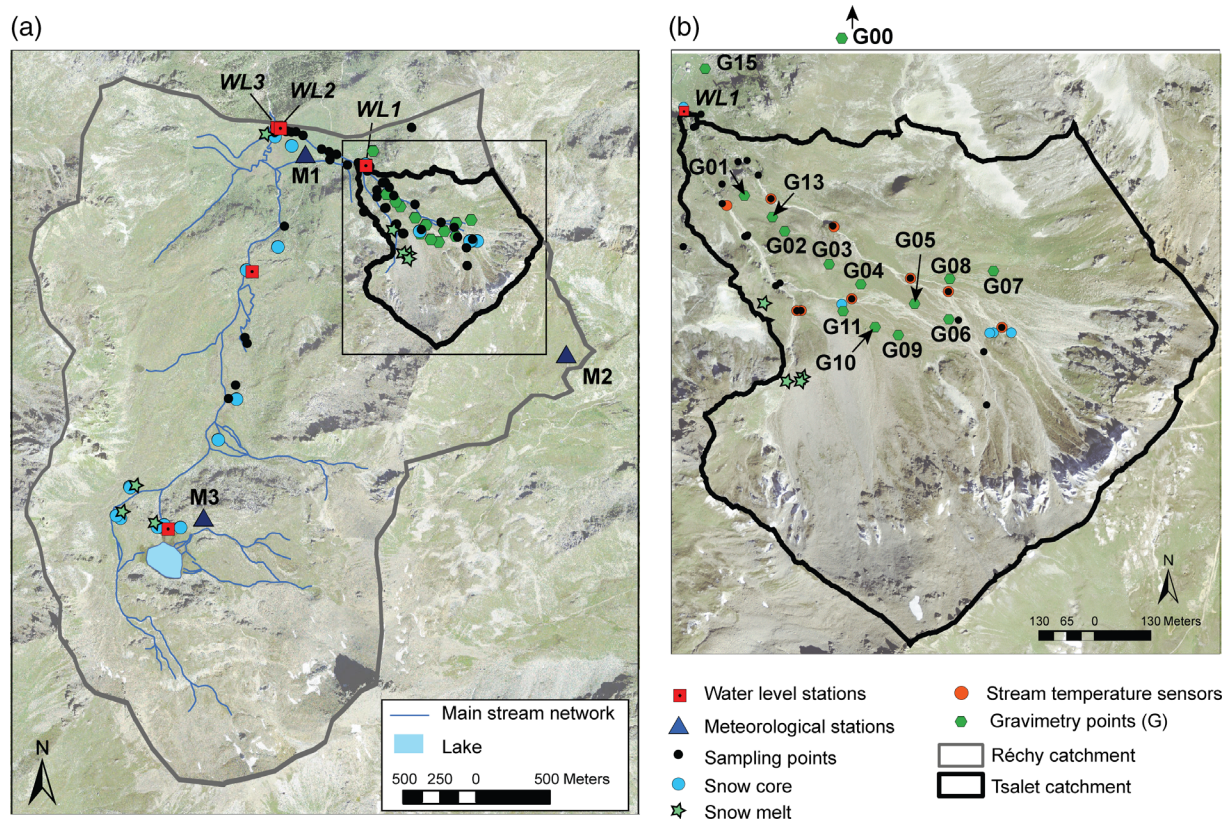


**FIGURE 1** Study site with the locations of observation points: (a) Réchy and Tsalet catchments and (b) zoom in on the Tsalet catchment; the background is a satellite image from SwissTopo (2015)

2,260 and 2,816 m a.s.l. with a mean altitude of 2,568 m a.s.l. It is located entirely above the tree line, has no glacial cover and the limited vegetation extent occurring during summer is presented in Figure 1b. Soil is mostly absent or very thin. Precipitation amounts to around 1,100 mm/year.

The Tsalet catchment belongs to the Pennine domain of the Alps. Rock outcrops mainly consist of quartzite, gneiss, calcschist and marbles. In the upper part of the catchment, evaporitic rock consisting of gypsum and cagneule outcrops are found (Challandes, 1992). Cagneule originates from the alteration of dolomite-bearing evaporites (Schaad, 1995). As a result of the action of glacial erosion, a step-like landscape has been formed consisting of a sequence of rock basins and riegel, as commonly encountered in alpine glacial valleys (Marthaler, Sartori, Escher, & Meisser, 2008). The slopes are partly covered by talus deposits, moraine, alluvial fans, and sediments. In the upper part, permafrost can occur along the ridges at altitudes above 2,700 m.a.s.l (Lugon & Delaloye, 2001).

### 3 | METHOD

#### 3.1 | Overview

In order to improve our comprehension of groundwater storage processes in alpine catchments, we employ multiple hydrological

investigation methods in this study. Temporal dynamics of surface water-groundwater exchange are informed by thermal and manual measurements of streams and springs which tell us the dates of flow cessation. In addition, stable isotopes of snow, rain, spring and stream water are used to determine the original sources of water within the catchment and to highlight hydrological dynamics. Meteorological and hydrological measurements enable the calculation of a seasonal groundwater storage water balance. Finally, time-lapse gravimetry is used to determine relative variations in groundwater storage in different areas of the catchment.

#### 3.2 | Meteorological and hydrological measurements

Meteorological parameters (temperature, precipitation, and barometric pressure) are recorded at two automatic weather stations (Figure 1). One is located at the Ar du Tsan plateau (M1, 2,193 m a.s.l.) and the other at Lake Louché (M2, 2,567 m a.s.l.). Humidity and radiation are not measured in the catchment. Instead, representative data are sourced from the Meteoswiss Evolène/Villa (EVO) weather station, located at 1825 m a.s.l., 9.4 km south of the Tsalet catchment.

To estimate streamflow, water levels are measured hourly at different points of the catchment with several self-logging pressure transducers (WL stations, Figure 1). Rating curves are established via

manual discharge measurements, which are performed during field campaigns using the slug injection of a salt in solution method (Moore, 2005) covering a wide range of discharge values.

Snow depth is measured at the M1 and M3 stations with an ultrasound sensor mounted over the snowpack, which measures the distance to the snow surface. The automatic meteorological station from the Institute for Snow and Avalanche Research (M3, Orzival; 2,640 m a. s.l.) is located on the east side of the Vallon de Réchy catchment (Figure 1a). Snow water equivalent (SWE) and snow depth have been measured in the field at the same locations as snow sampling (Figure 1).

Self-logging temperature sensors (Hobo Mx2201) were installed at nine locations in the flowing river during the melt period (Figure 1). These sensors allow the determination of the time when water at the location of the sensor is no longer flowing. In this case, the sensors record the air temperature, which remains higher than the water temperature. Water temperature measurements were carried out in the field using WTW probes to verify the sensor measurements. Additionally, in order to identify zones of groundwater discharge, an aerial survey was performed on the lower part of the Tsalet catchment using a SenseFly eBee drone with a thermoMAP thermal camera (relative precision 0.1 K; absolute accuracy 5 K). This survey was carried out in the afternoon of a summer day (July 24, 2019) with limited cloud cover resulting in contrastingly lower temperatures in zones of groundwater discharge.

### 3.3 | Water sampling of isotopic measurements

Water samples from streams and springs were collected and stored in 8 ml glass bottles for the measurement of the stable isotopic composition of water ( $\delta^{2}\text{H}$  and  $\delta^{18}\text{O}$ ). Samples to determine the isotopic composition of rainwater were collected in a rain collector located at M1 (Figure 1) designed to prevent water evaporation (Palmex Rain Sampler RS1). Melt samples were collected directly in the field in 5 ml glass bottles from melt runoff during the melt period (June 2019). Melt runoff was identified downstream from the snowpack, nine melt samples have been collected (Figure 1). For stream and spring sampling, four field campaigns are performed at four specific periods: during the snowmelt peak (June 28, 2019), at the beginning of the snow-free period (July 24, 2019), during the snow-free period (September 04, 2019), and the end of the snow-free period (October 17, 2019). The isotopic composition of snow was measured from snow cores collected in March 2019 and June 2019 at locations presented in Figure 1. Snow cores were extracted from the entire snow column as best as possible (sometimes a few centimetres were missing) using a SWE measurer (graduated cylinder and balance), then collected in closed bags and finally in glass bottles after melt while minimizing exchanges with the atmosphere. In total, 19 snow cores have been collected (Figure 1) at snow heights varying from 4.5 to 0.3 m.

Water stable isotopic compositions were measured with a Picarro spectrometer (L2130-i IRMS). Results are reported in  $\delta$  values, representing deviations in per mil (‰) from the isotopic composition of the international standard (Vienna Standard Mean Ocean Water,

VSMOW), such that  $\delta^{2}\text{H}$  or  $\delta^{18}\text{O} = (R_{\text{sample}}/R_{\text{VSMOW}} - 1) \times 1,000$ , where R refers to  $^2\text{H}/\text{H}$  or  $^{18}\text{O}/^{16}\text{O}$  ratios.

## 3.4 | Water balance

### 3.4.1 | General definition

In alpine catchments, an important part of the groundwater recharge occurs via snowmelt. In the study catchment, around 50% of precipitation occurs as snow and the snowmelt period causes an increase in groundwater storage (Cochand et al., 2019). Beyond the period of snowmelt, groundwater is the dominant source of water during dry periods. We calculate the subsequent seasonal groundwater storage depletion during the period of the high decrease in groundwater storage: from the end of snow cover (July 23, 2019) to the beginning of the snow accumulation period (October 14, 2019). Over this period the water balance is expressed as follows:

$$Q = P - E + \Delta S_{\text{GW}} \quad (1)$$

where  $\Delta S_{\text{GW}}$  is the seasonal groundwater storage change,  $P$  the precipitation,  $Q$  the stream discharge at the outlet of the catchment and  $E$  the evapotranspiration. As soils are absent or only very thin, we neglect changes in soil water storage. The melt of ground ice within the watershed is expected to be very low and not to influence the water balance.

### 3.4.2 | Quantification of water balance terms

#### Evapotranspiration

Evapotranspiration ( $E$ ) from vegetated areas is calculated using the equation from Priestley and Taylor (1972):

$$E = \alpha \frac{\Delta}{\Delta + \gamma} \frac{R_n - G}{L \rho_w} \quad (2)$$

where  $\alpha$  is a dimensionless parameter;  $\Delta$  ( $\text{kPa}/^\circ\text{C}$ ), the slope of vapour pressure curve;  $\gamma$  ( $\text{kPa}/^\circ\text{C}$ ), the psychrometric constant;  $R_n$  ( $\text{MJ m}^{-2} \text{day}^{-1}$ ), the net radiation;  $G$  ( $\text{MJ m}^{-2} \text{day}^{-1}$ ), soil heat flux;  $L$  ( $\text{MJ}/\text{kg}$ ), the latent heat of vaporization; and  $\rho_w$ , the density of water ( $\text{kg}/\text{m}^3$ ).  $R_n$  is estimated according to Allen, Pereira, Raes, and Smith (1998), parameters not measured at M1 station are estimated from the measurements at the EVO weather station.  $E$  is calculated on a daily basis.  $G$  is not measured in the field but was estimated to be 10% of daily  $R_n$  based on previous studies in alpine areas (Blanken et al., 2009; Hood & Hayashi, 2015). For the alpine environment,  $\alpha = 1$  is used to estimate evapotranspiration as suggested by various authors (Eaton, Rouse, Lafleur, Marsh, & Blanken, 2001; Hood & Hayashi, 2015; Saunders, Bailey, & Bowers, 1997). The calculated evapotranspiration is illustrated in Figure 2. Evapotranspiration from non-vegetated areas such as talus and bedrock is assumed to be

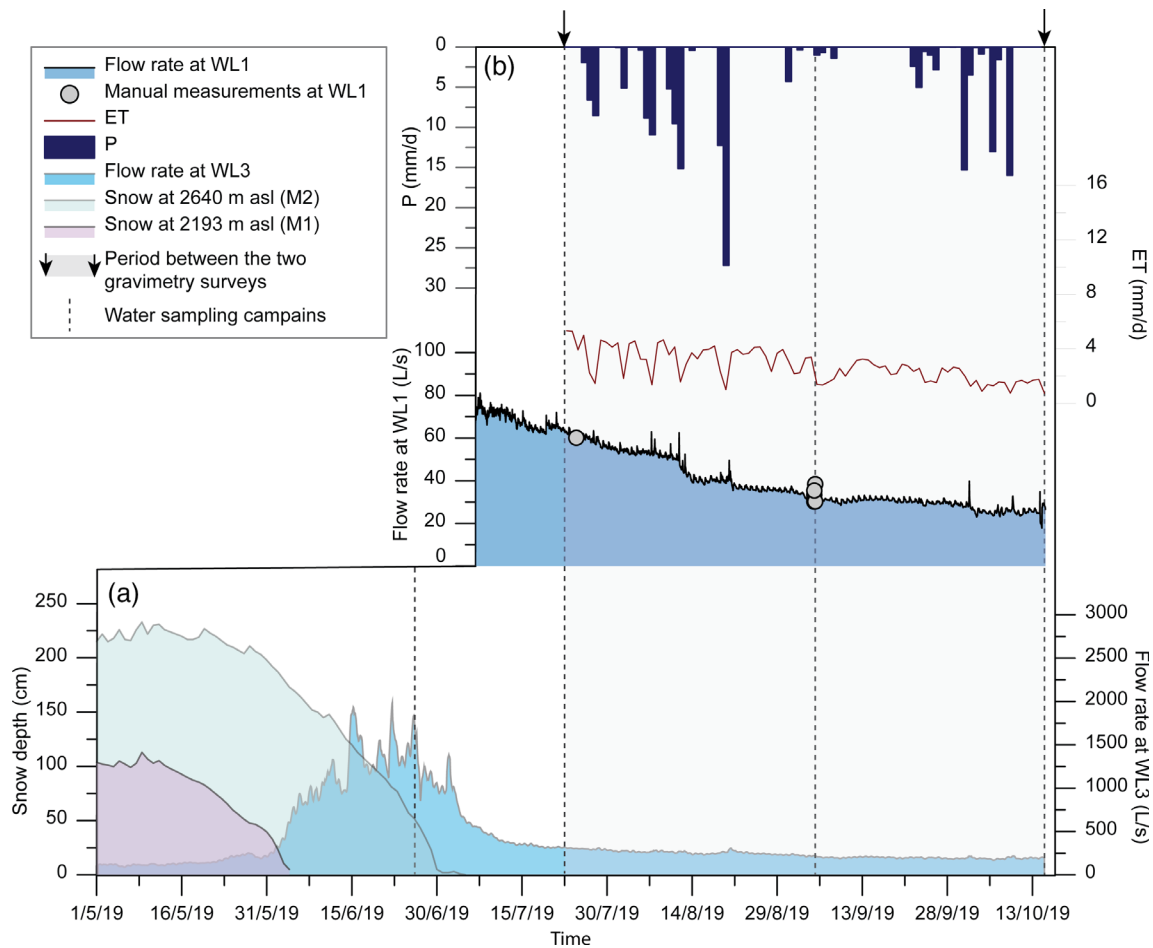


**FIGURE 2** (a) Illustration of the evolution of the snow depths at the M1 and M2 meteorological stations and the flow rate in the Rêche river (WL3 water level station) to illustrate the hydrological cycle between the maximum snow depth and the end of the snow-free period; (b) evolution of the terms of the water balance over the period between the two gravimetry surveys

negligible. Vegetation cover is estimated from satellite photography in summer 2015 and covers a surface area of 0.59 km<sup>2</sup> (Figure 1). The uncertainty of evapotranspiration is estimated to be 20%, based on error propagation following Cochand et al. (2019).

#### Flow rate

Because sediment accumulation caused the water level measurement at the WL1 station to fail for a part of the measurement period, we assume that the evolution of flow rate is similar between WL2 (Tsalet river downstream) and WL1 (Tsalet river upstream). The flow rates at both stations are correlated and therefore a linear regression is used to obtain the flow rate at WL1. The obtained discharge at WL1 over the targeted period is illustrated in Figure 2. Surface runoff at the catchment outlet (WL1) is quantified by integrating the continuous discharge time-series over time. Uncertainties associated with streamflow estimation are as follows: the uncertainty of water depth using a water level probe of 0.5%; that of the salt gauging method, 5% (Moore, 2005); and that of the rating curve, 20%. Given that these uncertainties are uncorrelated, total uncertainty is calculated using the root mean square propagation method, resulting in a value of 21%.

#### Precipitation

Precipitation is assumed to be equally distributed over the catchment and equal to precipitation measured at the M1 station (Figure 2). Uncertainty in rain measurements is expected to be 10% as under-catch can be 3% and the 4% gradient between M1 and M3 (Cochand et al., 2019) has not been considered.

#### Maximum snow water equivalent ( $SWE_{max}$ )

$SWE_{max}$  is not part of the water balance but is used to estimate the recharge potential on the catchment as it gives the quantity of water available during the melt period. We first estimate the maximum snow depth and then the  $SWE_{max}$ . The snow height is calculated based on a linear interpolation between the two meteorological stations measuring snow depth (M1 and M2; Figure 1 for locations and Figure 2 for snow depth measurements). The snow depth is extrapolated over the entire catchment using the digital terrain model (DEM, 25 m resolution), that is, at each elevation a value of snow height is known based on the linear interpolation between the two meteorological stations. A linear trend between snow height and altitude have already been observed in the Rechy catchment using LidAR measurement of snow

height in the previous study of Cochand et al., 2019. The SWE is calculated using a published empirical relationship between snow density, season, snow height, and altitude (Jonas et al., 2009). This relationship has been derived from 11,147 data records from 48 winters and 37 stations throughout the Alps. The relationship is expressed as follows:

$$\rho_{swe} = ah_{snow} + b + l \quad (3)$$

where  $\rho_{swe}$  is the apparent density of snow cover in  $\text{kg m}^{-3}$ ;  $a$  and  $b$ , the regression coefficient depending on altitude and month;  $h_{snow}$ , the measured snow depth; and  $l$ , a constant depending on the region ( $-1.1 \text{ kg m}^{-3}$  for our study site). The maximum snow depth and  $\text{SWE}_{\max}$  calculations are validated using manual measurements (Figure S1).

### 3.5 | Time-lapse gravimetry

#### 3.5.1 | General theory

Considering the Earth as a perfect sphere of mass  $M$  ( $5.972 \times 10^{24} \text{ kg}$ ), acceleration due to gravity,  $g$ , is:

$$g = \frac{F}{m} = \frac{GM}{r^2} \quad (4)$$

where  $G$  is the gravitational constant ( $6.674 \times 10^{-11} \text{ m}^3 \text{ kg}^{-1} \text{ s}^{-2}$ );  $m$ , the mass of a measured object; and  $r$ , the distance between the centre of mass of the Earth and the measured object. Taking the first derivative of  $g$  with respect to  $r$ , we obtain:

$$\frac{\partial g}{\partial r} = -\frac{2GM}{r^3} \quad (5)$$

At our study site (latitude  $\sim 46.2^\circ \text{N}$ , elevation  $\sim 2,400 \text{ m}$ ), for every  $1 \text{ m}$  of elevation gain,  $g$  will change by approximately  $-3.0849 \times 10^{-6} \text{ m/s}^2$  or  $-308.49 \text{ } \mu\text{Gal}$ , where  $1 \text{ Gal} = 0.01 \text{ m/s}^2$ . This is the so-called free-air correction and is needed here to compensate for small elevation differences between repeat measurements at the same location. The effect of local groundwater storage fluctuations on gravity can be modelled by considering the addition or removal of a layer of water from near the Earth's surface. This can be approximated by considering an infinite plane of thickness  $\delta h$  and density  $\rho_{\text{H}_2\text{O}} = 1,000 \text{ kg/m}^3$  which results in a change in gravity of:

$$\delta g = 2\pi G \rho_{\text{H}_2\text{O}} \delta h = \beta \delta h \quad (6)$$

where  $\beta = 4.193 \cdot 10^{-7} \text{ s}^{-2}$ . This is groundwater version of the Bouguer plate approximation. Thus, for a drop of groundwater storage of  $1 \text{ m}$ , gravity will decrease by  $\sim 41.9 \text{ } \mu\text{Gal}$ . Stated differently, a decrease in  $g$  of  $1 \text{ } \mu\text{Gal}$  corresponds to a decrease in local groundwater storage of  $\sim 2.38 \text{ cm}$ . Ignoring storage in the vadose zone, for a homogeneous

porous material of porosity,  $\epsilon$ , 0.4 this would correspond to a lowering of the water table by  $\sim 5.96 \text{ cm}$ . These calculations illustrate the precision required,  $<10^{-8}$  of  $g$  for groundwater table fluctuations of  $(23 \text{ cm})/\epsilon$ , when employing gravimetry for hydrogeological investigations. Under this approximation, Leirião, He, Christiansen, Andersen, and Bauer-Gottwein (2009) characterized the water "footprint" in the context of gravimetric measurements, noting that the radial extent of change in groundwater that contributes to 90% of the change in gravity is  $\sim 10 \text{ h}$ , where  $h$  is the depth to the water table.

Temporal and spatial corrections are required to obtain accurate gravimetric measurements. However, as time-lapse gravimetry is only concerned with changes in gravity over time at a given point, spatial corrections are significantly simplified. Most notably, terrain corrections (Li & Sideris, 1994) can be completely ignored as the only meaningful change in mass in proximity to a measurement point is assumed to be due to the transport of water. This assumption would, of course, not hold in the case of significant movement of solid material due to, for example, excavation or rockslides. In our study area no change in the location of solid material was observed.

#### 3.5.2 | Survey and equipment

The single-day gravimetry surveys were carried out at the end of the snowmelt period (July 23, 2019) and prior to the first snowfall (October 14, 2019) in the catchment. This 83-day period corresponds to a period when pronounced decline in streamflow in the Tsalet is observed and when the site is more easily accessible than in months when snowcover can be expected. The targeted zone encompasses the talus field and the moraine located between two ephemeral streams. These areas of the catchment are expected to have the highest seasonal variations in groundwater storage. The exact locations were chosen so as to form a loose transect along the topography gradient between stations G01 and G06 (Figure 1) with additional lateral points located elsewhere on the talus field.

Relative gravity measurements were carried out with a Scintrex CG-5 Autograv unit (Scintrex Ltd., 2012) which has a reading precision of  $1 \text{ } \mu\text{Gal}$ . The gravimeter is designed to carry out relative gravimetric measurements and can correct for a small range of tilt and also for Earth tides (ET) using the formula of Longman (1959). During the July survey, measurement locations were established using a Global Navigation Satellite System (GNSS) surveying unit (Leica GS-15). To assist in finding the surveyed positions during subsequent surveys, coloured metal stakes were driven into the ground at each location, although coordinates from the GNSS measurement locations suffice for localizing the positions. Positions were recorded for both the July and October surveys, enabling corrections for minor differences in elevation between the two surveys. For each measurement, a custom tripod stand was driven into the thin layer of topsoil and the adjustable gravimeter tripod placed upon it. For the October survey, the tripod positions of the July were located and the tripod reinstalled. The tilt of the gravimeter was finely adjusted prior to each measurement to ensure the device was upright according to standard procedure

(Scintrex Ltd., 2012). These steps assist in minimizing error due to ground settling during measurements. Multiple 30s repeats of each measurement were performed until five consecutive measurements within a range of  $<5 \mu\text{Gal}$  were recorded.

To enable drift correction during the surveys, station G00 near the village of Vercorin (1,322 m a.s.l.) was surveyed at the beginning and end of each survey (Figure 1). This location, although not an absolute gravity reference, provides our reference point for comparisons between the two surveys. Typical seasonal variations in groundwater levels in alpine catchments in Valais (Kimmeier, Bouzelboudjen, Ornstein, Weber, & Rouiller, 2001) show that any variation in the groundwater storage over the study period would be negative, that is, that it is not possible to have increasing groundwater storage during this period in this nival-regime hydrogeological setting. Station G15, located approximately 100 m from the bottom of the catchment, was surveyed at the beginning and the end of the surveys, while G04 served as a local reference station for drift corrections was returned to and measured four times, at intervals of approximately 90 minutes, during the surveys.

### 3.5.3 | Gravity data processing and uncertainty

A free-air correction was first applied to all gravimetric measurements using the elevation values ( $\pm 1$  cm) obtained from GNSS surveying, which differed by  $-10$  and  $5$  cm between surveys, corresponding corrections of  $-15$  to  $30 \mu\text{Gal}$  [Equation (5)]. The CG-5 gravimeter can automatically apply an ET correction using the formulas of Longman (1959). The accuracy of this correction was investigated by comparison with the output of pyGtide (Rau, 2019), a python wrapper for ETERNA (Wenzel, 1996; (Kudryavtsev, 2004). Inconsistencies up to  $7.5 \mu\text{Gal}$  between the two ET calculation methods were observed and thus finer ET corrections using output from pyGtide were applied.

The ET- and elevation-corrected gravimetric data was then drift-corrected, using the repeated stations G00, G15, and G04. Linear interpolation was used for stations G00 and G15 while cubic interpolation was used for station G04 due to it being measured four times. For each survey, the raw  $g$  values were corrected for elevation and ET before applying the drift calculation. This ensures that the only factor in the drift correction other than noise affecting the difference in repeat measurements of a given location in a given survey was instrumental drift. After applying elevation, ET, and drift corrections, the difference in the relative gravity values from the July and October 2019 surveys was calculated.

There are three main contributors to uncertainty in the time-lapse gravimetric measurements: instrumental precision, elevation measurement precision, and instrumental drift. Instrumental precision incorporates contributions from the instrumental reading precision ( $\pm 1 \mu\text{Gal}$ ) and variations related to internal vibration, tilt, and temperature corrections in the CG-5. As five repeat measurements within a range of  $5 \mu\text{Gal}$  were made for each measurement point, we estimate a conservative instrumental precision of  $\pm 3 \mu\text{Gal}$ . Elevation was measured to  $\pm 1$  cm for each measurement, which corresponds to an uncertainty of  $\pm 3 \mu\text{Gal}$ . As both the instrumental precision and elevation uncertainty

will affect the drift corrections, we estimate a drift uncertainty of  $\pm 4 \mu\text{Gal}$ , obtained from the sum of squares of the aforementioned uncertainties. The total uncertainty on the measurements of a single survey is therefore  $\pm 6 \mu\text{Gal}$ . As the values of interest here are the difference between the two surveys, we multiply this value by  $\sqrt{2}$  to obtain a final time-lapse gravity uncertainty of  $\pm 8 \mu\text{Gal}$ .

## 4 | RESULTS AND DISCUSSION

### 4.1 | Evolution of drying springs and streams highlighted by field observations

In order to develop a conceptual model of the hydrology of the Tsalet catchment, the spring and stream drying sequence is investigated and the results are presented in Figure 3a. In June, streams and springs are flowing at their highest flow rate. The snowmelt peak occurred at the end of June (Figure 2) and by July, almost all of the snow cover had melted, with only a few small snow patches remaining. The results of the temperature sensors (Bn; Figure 3a) show that the streams upstream i4, on the west part, and above i7, on the east part, stop flowing between 2 and 15 July, following the evolution of the snow cover. Thus, on the upper part of the catchment, almost all streamflow has ceased except a small one (flow rate  $< 1$  L/s) measured by i1, i2 and i3 (Figure 3a). This small stream springs from underneath a small snowpack and disappears after i3 by infiltrating in unconsolidated deposits. Further down-gradient, streams are flowing in July at i4 (0.9 L/s) and i7 (4.3 L/s). At i7, multiple springs give rise directly to the Tsalet stream. The thermal image (Figure 3b; captured the July 23, 2019) shows in more detail the locations of the springs. It is interesting to observe that the spring S2 belongs to a larger spring complex located west of S2, hidden under vegetation in the field. In addition, several springs discharge in the river channel at i7, explaining the continuous flow and down slope B8 with lower flow rate. Finally, in October, all previous stream upstream i7 (1.6 L/s) and i9 (0.5 L/s) are dry and all streams below are still flowing. At this date, the spring S1 is also dry, whereas the spring S2, located slightly lower, is still flowing. These dynamics highlight two different hydrogeological systems: a shallow one, located on the upper part of the catchment, fed directly by snowmelt and rapidly depleted, and a deeper one with a slower recession, emerging at the lower part of the catchment from deeper groundwater flows. On the surface, the first system has a strongly retracting stream network.

### 4.2 | Early and late snowmelt influences highlighted by stable isotopes of water

#### 4.2.1 | The isotopic composition of rain and snow

Unsurprisingly, the isotopic composition of rainwater is enriched compared to the other components, with a mean  $\delta^{18}\text{O}$  ranging from  $-6.9$  to  $-7.5 \text{‰}$  between June and September and a mean of  $-10.6 \text{‰}$

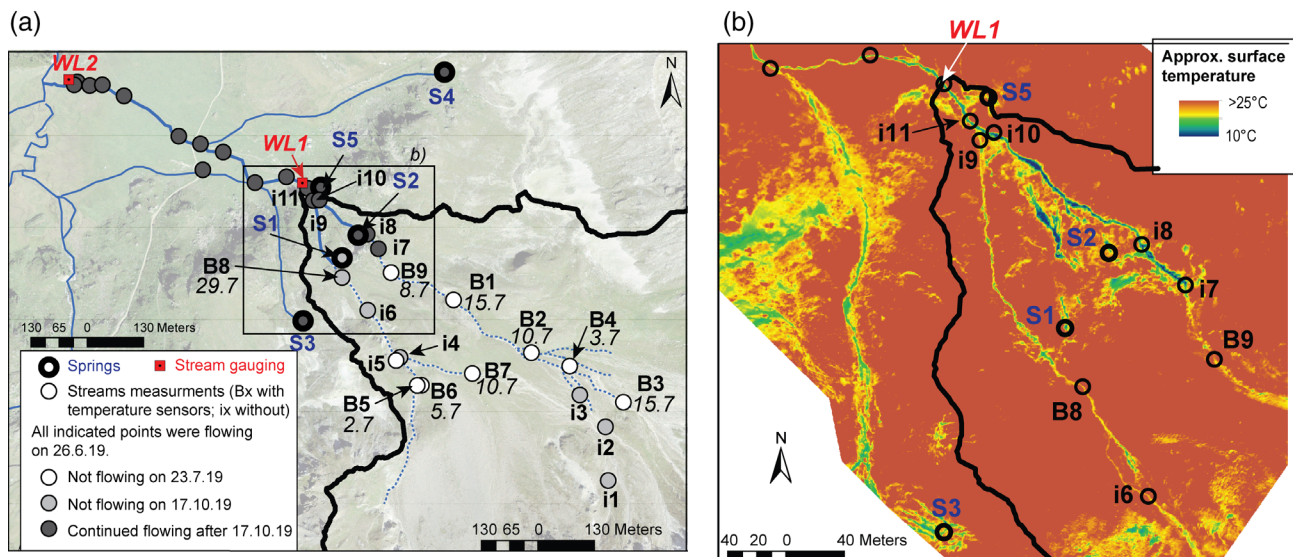


**FIGURE 3** (a) Evolution of drying springs (S1-4) and streams (i1-11, B1-9 and WL1-2), based on observations from the field campaigns and results of self-logging temperature sensors (B1-9): the dates (day month) indicate the date of drying up of the sensors (the 'B' labels indicate water sample points with self-logging temperature sensors, the 'i' points are only sample points, without temperature sensors); (b) thermal image recorded 23.7.2019, zoom on the perennial spring area of the catchment

between September and mid-October (Figure 4). The isotopic composition of snow and melt is more surprising as the mean  $\delta^{18}\text{O}$  of snow core samples varies between  $-16.0$  to  $-14.5$  ‰ in March and between  $-13.4$  and  $-10.4$  ‰ in June, this last value being close to the isotopic composition of the rain in October (Figure 4(a)). Similarly to the snow in June, the sampled meltwater from June has an isotopic composition ranging from  $-13.5$  to  $-11.8$  ‰.

In theory, the isotopic composition of snow is significantly more depleted than other waters (Beria et al., 2018). However, melt processes and snow transformation can lead to an enrichment of the snowpack (Dietermann & Weiler, 2013). It has been shown that an enrichment of heavy isotopes in the upper snow layers takes place due to diffusion of water vapour in the pores of the snowpack and also partial melting, which causes evaporation and percolation of meltwater in the remaining snow (Gat, 1996; Stichler et al., 2001) as well as kinetic fractionation occurring during sublimation (Biederman et al., 2014; Gustafson, Brooks, Molotch, & Veatch, 2010). In addition, enriched water from precipitation during spring can percolate through the snowpack. Furthermore, it has already been observed in the Austrian Alps, that, during the snowmelt period, fractionation processes proceed and the snowpack becomes more homogenous, leading to a gradual isotopic enrichment of the snowpack (Schmieder et al., 2016). This temporal variability in snowmelt and snowpack isotopic composition is greater for the north-facing slope compared to the south-facing slope (Schmieder et al., 2016). The Tsalet slopes are mainly north-facing and similar processes are observed.

#### 4.2.2 | The isotopic composition of groundwater

It is interesting to note that groundwater coming from the springs has an isotopic composition ranging between  $-14.8$  and  $-14.1$  ‰. This

composition remains stable during the four sampling campaigns, meaning that the water originates from deeper infiltration with a mean isotopic composition reflecting recharge processes over a longer period. In addition, their isotopic composition is more depleted than meltwater in June (just after the melting peak). It means that the meltwater recharging groundwater feeding the springs likely comes from earlier meltwater, stemming mostly from the snowmelt peak. Therefore the earlier melt is more effective to recharge the depleted groundwater system after long period without recharge during winter. Even if more years of melt and snow sampling would be needed to validate this assumption, the clear differentiation between springs and late melt (from late June to July) allows us to highlight two different hydrological systems: late melt dominated ones and groundwater (i.e., earlier melt) dominated ones.

#### 4.2.3 | Isotopic composition of streams

The two groups of stream samples identified in Section 4.1 are clearly identifiable: (a) the upper group samples which dry rapidly, are more enriched in water stable isotopes, and are in the range of late meltwater isotopic composition (i.e., sample points located above i7 and B8: from i1 to i6, from B1 to B7 and B9; Figure 3 and upper group in Figure 4); (b) the lower stream group, located below the springs, which are groundwater-dominated with isotopic compositions close to spring isotopic composition (from i7 to i11, B8, WL1, WL2 and between them; Figure 3 and intermediate and lower groups in Figure 4). The stream samples B8 and i9, located below the springs, vary from late snowmelt-dominated to groundwater-dominated between the campaigns (Figure 4). The isotopic compositions of the stream water located above the springs become more enriched from

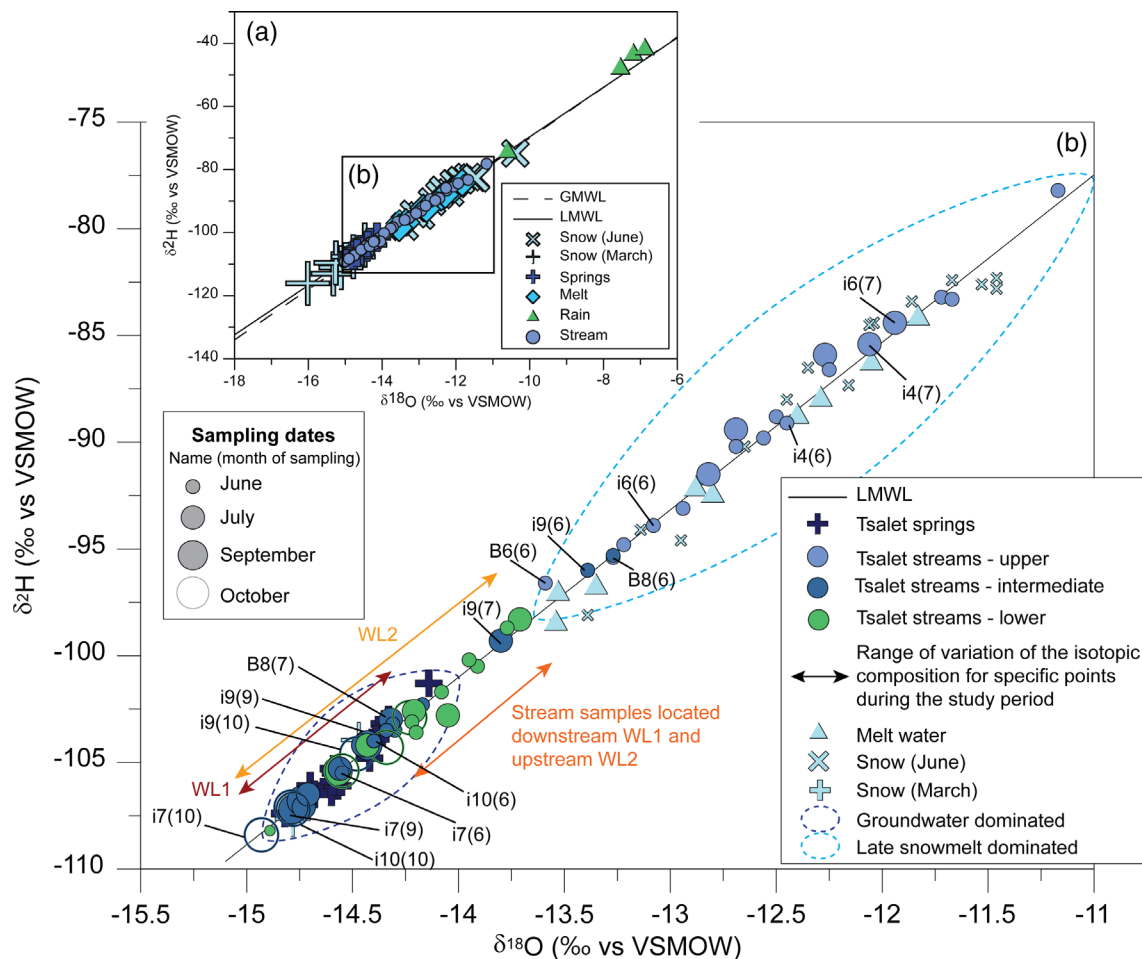


**FIGURE 4** Isotopic composition of streams, springs and rain measured during the four campaigns (26.6.2019, 23.7.2019, 04.09.2019 and October 17, 2019), snow cores measured in March and June 2019 and snowmelt measured in June 2019. The corresponding locations of the samples are illustrated in Figure 3; (a) all water samples and (b) zoom in on stream and spring samples, only labels of water points still flowing in July are presented to illustrate the evolution of isotopic composition and therefore water origin in time (the 'B' labels indicate water sample points with self-logging temperature sensors, the 'i' points are only samples points, without temperature sensors); for clarity, results for water samples below WL1 are represented by an arrow showing the range of variation over the study period

June to July (for the ones which are still flowing, for example i6 and B6; Figure 4) because of more enriched snowmelt influence. In contrast, stream water located below the springs becomes more depleted and has isotopic compositions closer to those of the spring because of less water coming from snowmelt (for example B8, i6, i8, i9 i10; Figure 4). It is also interesting to observe that downstream at the WL1 location, located itself just below the spring area, the isotopic composition increases again, probably due to influence of other late snowmelt-dominated streams arriving in the Tsalet and the possible re-infiltration of the Rêche which can have more enriched isotopic composition due to late snowmelt influences in the Réchy catchment.

These results show that the springs located below the talus and moraine of the Tsalet catchment where bedrock is exposed (Figure 5) feed the majority the Tsalet catchment and allow flow to be maintained during the entire year. This occurs even during long winter low-flow periods, whereas late snowmelt dominated streams are ephemeral, lasting between a few days and 5 weeks after snowmelt peak. These

dynamics confirm the high variability of storage in the talus and moraine aquifers and the existence of slower hydrogeological systems feeding the springs and mainly recharged by water of the snowmelt peak.

### 4.3 | Seasonal groundwater storage changes calculated with water balance

Over the targeted period (July 23, 2019–October 14, 2019) mean water inputs in the catchment are  $182 \pm 18$  mm of precipitation and mean outputs are an ET of  $126 \pm 25$  mm and a surface flow rate of  $339 \pm 68$  mm (Table 1). Assuming that there is no other inflow or outflow within the catchment, and therefore that the groundwater catchment is the same as the topographic one, the storage loss amounts to  $283 \pm 111$  mm. The  $SWE_{max}$  in 2019 is estimated to be 849 mm over the catchment. Therefore these 2.6 months of groundwater loss represent 27% of the recharge potential on the catchment  $SWE_{max}$ .

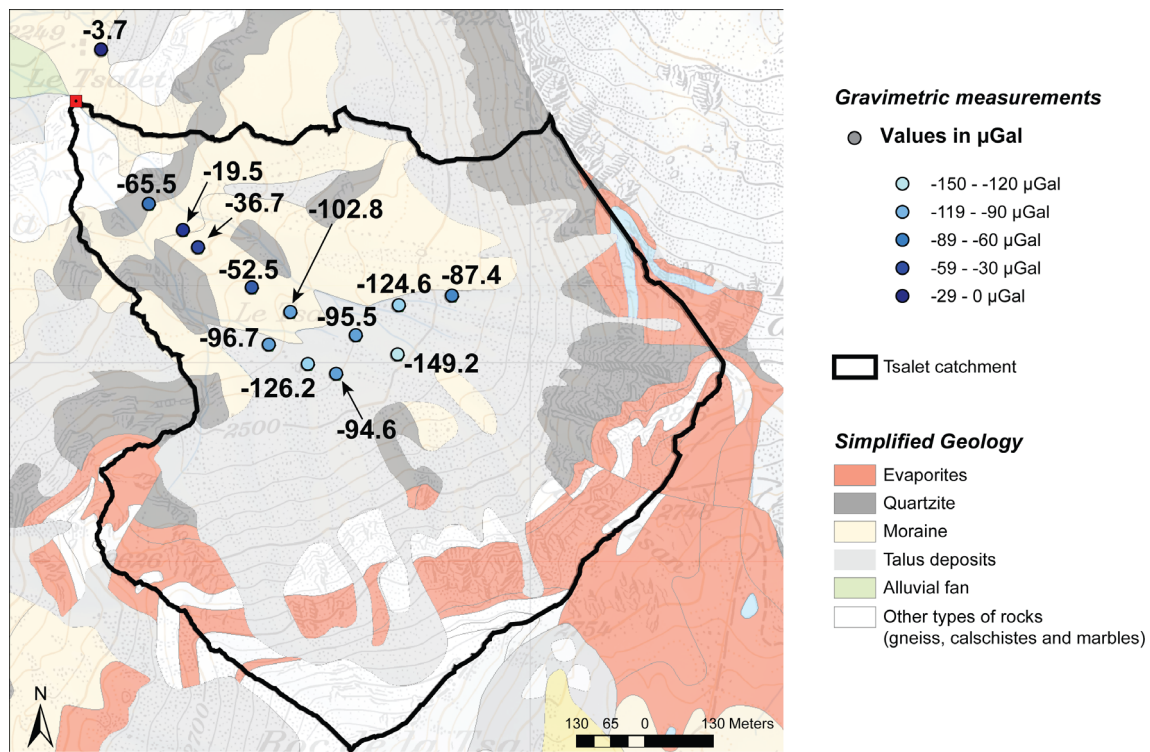


**FIGURE 5** Results obtained from the two gravimetry surveys and simplified geology of the Tsalet catchment derived from the Swiss geological map 1:25,000 (SwissTopo, 2018)

**TABLE 1** Water balance over the targeted period: precipitations (P), evapotranspiration (E), outflow (Q) and decrease in groundwater storage ( $\Delta S_{\text{GW}}$ )

P (mm)	E (mm)	Q (mm)	$\Delta S_{\text{GW}}$ (mm)
$182 \pm 18$	$126 \pm 25$	$339 \pm 68$	$283 \pm 111$

In their study involving the entire Réchy catchment, (Cochand et al., 2019) found a storage loss of  $150 \pm 40$  mm over the same period in 2013 with a  $\text{SWE}_{\text{max}}$  of  $660 \pm 32$  mm. They found that the part where the Tsalet catchment is located represents 30% of groundwater storage, therefore 113 mm on a  $2.5 \text{ km}^2$  area. The chosen zone appears to be a major contributor of groundwater storage in the larger Réchy catchment.

#### 4.4 | Spatial variations in groundwater storage changes highlighted by gravimetry

A decrease in gravity relative to that at the reference point G00 is observed at all investigated points within the Tsalet catchment. The time-lapse gravimetry results (Figure 5) display a clear trend with elevation. The relative decrease in gravity is most pronounced at higher elevations where the superficial layer of talus deposits is located. The values in this layer range between  $-87$  to  $-149 \mu\text{Gal}$ , indicating a significant decrease in groundwater storage. The magnitude of the  $\delta g$

values further downslope of the talus deposit area are generally smaller, ranging from  $-19.5$  to  $-105 \mu\text{Gal}$  in the moraine. Finally,  $\delta g$  at G15, the measurement location near the lower bound of the Tsalet catchment, is the only value falling within the calculated uncertainty range ( $\pm 8 \mu\text{Gal}$ ), indicating that the change in storage here, relative to that at G00, is negligible.

Using the simplistic infinite plane approximation [Equation (6)], the range of decrease in gravity for the measurements corresponds to a range of  $-2.08$  to  $-3.55$  m water equivalent in the talus and  $-0.46$  to  $-2.45$  m water equivalent in the moraine. While the true change in water levels beneath our gravimetric measurement locations can differ from these values, these values provide indicative values of the relative changes in groundwater storage in the moraine and talus. With regards to uncertainty in the conversion of  $\delta g$  values to water equivalent, the value of  $\beta$  in Equation (6) for any given measurement location above non-planar water tables and those with non-uniform changes can vary. For example, for a measurement point on significantly flatter topography than that of the Tsalet catchment, Creutzfeldt, Güntner, Klügel, and Wziontek (2008) determined a value of  $\beta = 5.249 \times 10^{-7} \text{ s}^{-2}$  (i.e., 1.905 cm of water equivalent for  $\delta g = 1 \mu\text{Gal}$ , 20% less than the value used for the conversions in Figure 5) cautioning that quantitative interpretation of time-lapse gravimetry measurements requires additional hydrogeological measurements. In order to precisely calculate effective water equivalents from  $\delta g$  measurements, one would require information on the depth of the water table throughout the catchment which could then be fed into a 3D gravimetric model (Leirião et al., 2009). Even though gravimetric

measurements are not a one-for-one substitute for hydraulic head measurements, they still provide valuable information on the relative changes in groundwater storage across different zones of interest.

The large  $\delta g$  values obtained in the Tsalet catchment indicate significant fluctuations in groundwater storage between July and October, with the largest decreases occurring in the talus field. Only one other study (McClymont et al., 2012) using time-lapse gravimetry to study seasonal changes in alpine groundwater storage is known to exist, although the hydrogeological conditions at their Lake O'Hara catchment site in the Canadian Rocky Mountains are significantly different from those in the Tsalet. The authors applied time-lapse gravimetry at dates in the annual hydrological cycle (July and September) similar to those of our study but obtained smaller  $\delta g$  values between  $-25$  and  $+8 \mu\text{Gal}$  in a moraine-talus field. Their gravimetric measurement points spanned  $\sim 50$  m in elevation range over  $\sim 750$  m horizontal meters of undulating topography and pore ice was present in a large portion of the studied site, reducing effective porosity. In the Tsalet talus field, our measurements spanned  $\sim 50$  m of elevation range over a maximum horizontal distance of  $\sim 350$  m, with a constant slope of  $\sim 19\%$  calculated between points G05 and G06 (Figure 1). The average slope between measurement locations G01 and G03, which are located on the moraine layer below the talus, is  $\sim 37\%$  (Figure 5). This implies that elevation-induced groundwater head gradients will be approximately twice as high in the moraine as in the talus for the investigated locations. While no measurements of the hydraulic properties of the talus and moraine in the Tsalet catchment exist, it is well-established that talus is significantly more permeable than moraine. For example, in the Canadian Rockies, Muir, Hayashi, and McClymont (2011) observed that talus has a very high hydraulic conductivity (0.01 to 0.03 m/s) and limited storage capacity to a time-scale of less than a week. Conversely, moraines have been regularly observed to have lower hydraulic conductivities in the approximate ranges of  $10^{-6}$  to  $10^{-4}$  m/s for lateral moraines and  $10^{-5}$  to  $10^{-4}$  m/s

for frontal moraines (Vincent, Violette, & Aðalgeirsdóttir, 2019). Thus, as moraine has a generally a lower hydraulic conductivity and lower porosity than talus (Hayashi, 2020; Vincent et al., 2019), groundwater flow rates in the moraine will be smaller, while larger and more rapid changes in groundwater storage will occur in the talus. In addition, these two systems can be connected and the groundwater depletion in the upper system (talus) can supply the lower system (moraine) leading likely to a smaller decrease of the water level.

#### 4.5 | Synthesis

The range of  $\delta g$  values observed implies significant decreases in water storage over a small portion of the catchment, implying that the survey has captured the preferential zone for fluctuations in groundwater storage. The seasonal groundwater storage decreases appear to be primarily focused in the talus, with an additional contribution from the moraine. The high discrepancies between storage variations measured with the gravimetry method ( $-2.08$  to  $-3.55$  m water equivalent in the talus and  $-0.46$  to  $-2.45$  m water equivalent in the moraine) and the water balance (storage loss of  $0.28 \pm 0.11$  m) could be partly explained by a difference between the topographically defined catchment and the hydrogeological catchment meaning that the surface outlet does not capture all the water flowing out of the catchment. The south-east orientation of the evaporite layers and the fracturing of the quartz basement could lead to an underestimation of the outflow from the Tsalet watershed and thus an underestimation of the loss of groundwater storage with the water balance method. However, it is unlikely that the groundwater storage decrease could be greater than the recharge potential corresponding to the amount of snow available for melting (0.85 m) or the total precipitation over the year (around 1.10 m). These values imply that the change in groundwater storage as determined through time-lapse gravimetry is likely

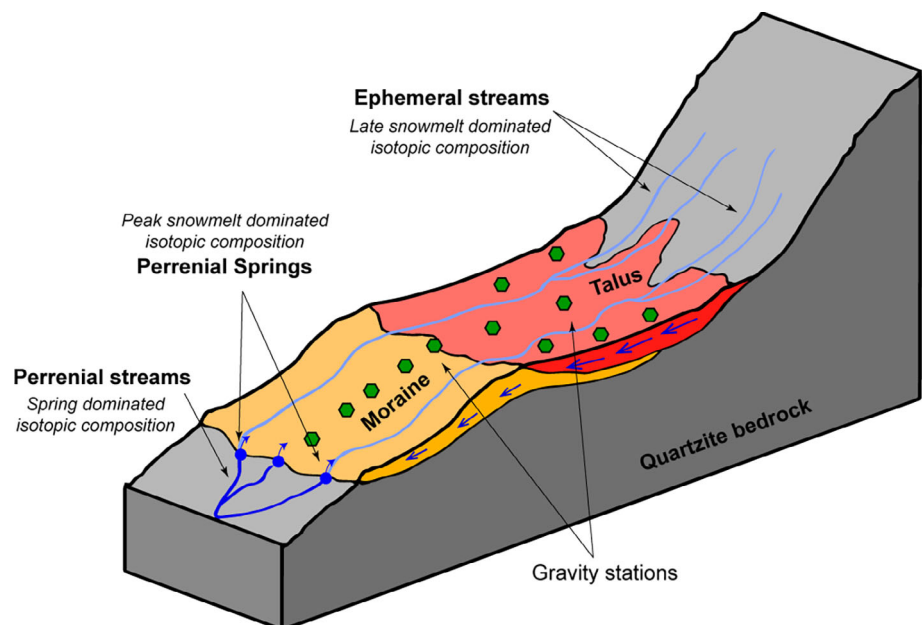


**FIGURE 6** Schematic diagram of the hydrogeological processes during the post-melt period in a talus and moraine snow-dominated catchment typical of the alpine regions

greater than the true value. Some uncertainties are associated with both methods to quantify the storage loss. In particular, the lack of a 3D gravity model, beyond the scope of this work, and an absolute reference station, render this application of time-lapse gravimetry primarily qualitative in its usage. Also, the fact that gravitational measurements do not target a specific point, but are rather inverse square-weighted averages, must be taken into account. Nonetheless, gravimetry results clearly demonstrate that high variations in groundwater storage occur in the talus, which has a very fast storage recession and contributes directly to outflow for a limited time (~1 month as illustrated by the drying streams and isotopic measurements). After this period where the talus is mostly drained, the moraine contributes significantly to storage loss and has a slower recession time due to its lower permeability, as summarized in the conceptual model in Figure 6. These findings agree with the conclusions of previous studies, indicating the important role of talus-moraine features in controlling groundwater storage and release. The recent study of Christensen et al. (2020) explored the role of moraine as a "gate-keeper" in one of these features in the Canadian Rockies, talus being located upslope of the moraine. In the Tsalet catchment, moraine likely plays this role as well. The bedrock, appearing at the surface downslope of the moraine where the springs are, also likely plays a "gate-keeper" role. In addition, we identify two types of groundwater dynamics: a shallow fast system, mostly occurring during snow melt and a deeper and slower system, assuring the water supply during the entire year. This confirms what has been shown from previous studies in alpine areas (Langston et al., 2011; Roy & Hayashi, 2009; or Pauritsch et al., 2016). The gravimetry results are complementary to the water balance and geochemical results because they enable confirmation of the difference in groundwater storage changes between aquifers units. These results illustrate that the combination of aquifer units is a key factor in alpine hydrogeology.

In addition to higher precisions associated with all terms, water balances require accurate estimations of groundwater catchment, which is not straightforward to determine in alpine areas where the geology is highly heterogeneous. Time-lapse gravimetry can be recommended for the identification of aquifers with high dynamic storage, although its use as a quantitative tool to accurately calculate changes in water volumes in alpine catchments likely requires a more elaborate approach. Quantitative use of time-lapse gravimetric measurements could be improved through the use of 3-d gravimetric modelling, absolute gravimetric stations and piezometers located in the targeted zone.

## 5 | CONCLUSIONS

Alpine areas have a major role in water supply in downstream valleys by releasing water during warm and dry periods. However, their hydrogeology is not well known and very exposed to climate change therefore improving our knowledge of alpine hydrogeological processes is of high importance today. The objectives of this study were to use a suite of methods to characterize seasonal groundwater

storage variations during a period of significant changes in an alpine catchment and, in turn, to improve our comprehension of groundwater storage processes in alpine catchments. The complementarity of the methods is both qualitative and quantitative, which each method providing spatial or temporal information (or both) needed to establish a conceptual hydrogeological model of the catchment. The water balance provides quantitative information about groundwater storage changes at the catchment scale. This method has been combined with methods that provide indication about the spatial variability of storage depletion. This includes gravimetry and a mapping of drying out of springs and contracting of the stream network. In addition, thermal UAV imagery provided qualitative spatial information on the locations of springs and water-saturated zones. Finally, the origin of the water that exits from the aquifer (former meltwater and/or rain water) and its variation in time is given by isotopic measurements.

Alpine regions such as the investigated Tsalet catchment have steep slopes and many small, interconnected aquifers. We have shown how gravimetric measurements can provide important hydrogeological information in alpine catchments, areas where instrumentation and monitoring are often challenging due, in part, to accessibility issues. When deployed in the post-snowmelt period, time-lapse gravimetric measurements enable rapid localisation of zones of seasonal groundwater storage changes. Nonetheless, the above-outlined challenges in studying alpine catchments also hinder the interpretation of gravimetric measurements via direct conversion to water equivalents. We recommend that gravimetry be complemented by other methods in order to characterize hydrogeological processes occurring in alpine catchments.

We have shown that temperature sensors enabled measurement of the temporal trend in stream and spring drying, providing valuable information about the time-scale of groundwater flow through the talus and the moraine. Stable isotope measurements allowed us to confirm the origin of surface water exiting the catchment and helped to inform our conceptual model. These results improve our comprehension of the conceptual schema highlighting two different hydrogeological systems: 1) a shallow one fed directly by snowmelt and rapidly depleted and 2) a deeper one, with a slower recession, emerging at the lower part of the catchment below the talus and moraine of the Tsalet catchment where bedrock shows up. These two types of flows confirm what has been shown from previous studies in alpine areas (Langston et al., 2011; Roy & Hayashi, 2009; or Pauritsch et al., 2016). The interaction between these two systems is probably that groundwater depletion in the upper talus system supplies the lower moraine system leading to a smaller decrease of the water level, the variations in groundwater storage being also conditioned by the differences in permeability between the two layers. The deeper system is isotopically stable and fed by the main recharge during peak snowmelt. The springs from this system feed the lower Tsalet catchment, enabling continuous flow during the entire year. These dynamics confirm the high variability of storage in the talus and moraine aquifers and the existence of slower hydrogeological systems feeding the springs and mainly recharged by the water of the snowmelt peak. Finally, gauging and meteorological measurements allowed the

calculation of a water balance, although the amount of water leaving the catchment as groundwater stays unknown. The seasonal groundwater storage calculation highlights the high contribution of the Tsalet catchment for the storage of the larger Réchy catchment, as hypothesized by Cochand et al. (2019).

Finally, these results highlight the dominant role of Quaternary deposits to store water. The mechanisms explaining the importance of Quaternary deposits are the combination of moraine and talus with different permeabilities allowing the storage of enough water to release it slowly during drier years, as stated in the publications of Cochand et al. (2019), Glas et al. (2019), Hayashi (2020), and Christensen et al. (2020). The high permeability of talus allows for the rapid infiltration of water and its connection to lower permeability moraine leads to deeper infiltration and a slower release of groundwater to streams, ensuring year-round streamflow down-gradient. Now, some more field measurements, such as piezometers, are needed to validate our conceptual model. Furthermore, the conclusions of our study can be applied to other alpine regions as unconsolidated Quaternary deposits are found in all alpine regions and the dynamics associated with snowmelt are similar.

## ACKNOWLEDGMENTS

This work was partly funded by the FOEN, within the framework of climate change impacts on water resources in Switzerland (HydroCH2018). We would like to acknowledge Meteoswiss, the Centre for research in alpine environment (CREALP) and the Institute for Snow and Avalanche Research (SLF) for providing us hydrological and weather data and SwissTopo for topographic and geological maps. We would like also to acknowledge Eric Travaglini, Roberto Costa, Jean-Michel Perruchoud and Laurent Marguet for their field support and Marion Cochand for her support on the previous knowledge and monitoring of the Réchy catchment. We thank Grégoire Mariéthoz for his drone which allow us to obtain the thermal images. We thank Masaki Hayashi and two anonymous reviewers for their review of our manuscript and their interesting and constructive comments.

## DATA AVAILABILITY STATEMENT

The data that supports the findings of this study are available in the supplementary material of this article.

## ORCID

Marie Arnoux  <https://orcid.org/0000-0002-2089-959X>

## REFERENCES

- Allen, R. G., Pereira, L. S., Raes, D., & Smith, M. (1998). *Crop evapotranspiration—Guidelines for computing crop water requirements*, (D05109). Roma: FAO.
- Ardelean, A. C., Onaca, A., Urdea, P., & Sarasan, A. (2017). Quantifying postglacial sediment storage and denudation rates in a small alpine catchment of the Fagaras Mountains (Romania). *Science of the Total Environment*, 599–600, 1756–1767. <https://doi.org/10.1016/j.scitotenv.2017.05.131>
- Barnett, T. P., Adam, J. C., & Lettenmaier, D. P. (2005). Potential impacts of a warming climate on water availability in snow-dominated regions. *Nature*, 438(7066), 303–309. <https://doi.org/10.1038/nature04141>
- Beniston, M., & Stoffel, M. (2014). Assessing the impacts of climatic change on mountain water resources. *Science of the Total Environment*, 493, 1129–1137. <https://doi.org/10.1016/j.scitotenv.2013.11.122>
- Beria, H., Larsen, J. R., Ceperley, N. C., Michelon, A., Vennemann, T., & Schaeffli, B. (2018). Understanding snow hydrological processes through the lens of stable water isotopes. *Wiley Interdisciplinary Reviews: Water*, 5(6), e1311. <https://doi.org/10.1002/wat2.1311>
- Biederman, J. A., Brooks, P. D., Harpold, A. A., Gochis, D. J., Gutmann, E., Reed, D. E., ... Ewers, B. E. (2014). Multiscale observations of snow accumulation and peak snowpack following widespread, insect-induced lodgepole pine mortality. *Ecohydrology*, 7(1), 150–162. <https://doi.org/10.1002/eco.1342>
- Blanken, P. D., Williams, M. W., Burns, S. P., Monson, R. K., Knowles, J., Chowanski, K., & Ackerman, T. (2009). A comparison of water and carbon dioxide exchange at a windy alpine tundra and subalpine forest site near Niwot ridge, Colorado. *Biogeochemistry*, 95(1), 61–76. <https://doi.org/10.1007/s10533-009-9325-9>
- Bucki, A. K., Echelmeyer, K. A., & MacInnes, S. (2004). The thickness and internal structure of fireweed rock glacier, Alaska, U.S.A., as determined by geophysical methods. *Journal of Glaciology*, 50(168), 67–75. <https://doi.org/10.3189/172756504781830196>
- Challandes, A. (1992). *Géologie générale et structurale dans le Sud et Ouest du val de Réchy (Pennique, Valais-Suisse) [general and structural geology in the southern and western part of the Réchy valley (Pennine, Valais-Switzerland)]*. Neuchâtel, Switzerland: Université de Neuchâtel.
- Christensen, C. W., Hayashi, M., & Bentley, L. R. (2020). Hydrogeological characterization of an alpine aquifer system in the Canadian Rocky Mountains. *Hydrogeology Journal*, 28(5), 1871–1890. <https://doi.org/10.1007/s10040-020-02153-7>
- Clow, D. W., Schrott, L., Webb, R., Campbell, D. H., Torizzo, A., & Dornblaser, M. (2003). Ground water occurrence and contributions to Streamflow in an alpine catchment, Colorado front range. *Groundwater*, 41(7), 937–950. <https://doi.org/10.1111/j.1745-6584.2003.tb02436.x>
- Cochand, M., Christe, P., Ornstein, P., & Hunkeler, D. (2019). Groundwater storage in high alpine catchments and its contribution to Streamflow. *Water Resources Research*, 55(4), 2613–2630. <https://doi.org/10.1029/2018wr022989>
- Cras, A., Marc, V., & Travi, Y. (2007). Hydrological behaviour of sub-Mediterranean alpine headwater streams in a badlands environment. *Journal of Hydrology*, 339(3–4), 130–144. <https://doi.org/10.1016/j.jhydrol.2007.03.004>
- Creutzfeldt, B., Güntner, A., Klügel, T., & Wziontek, H. (2008). Simulating the influence of water storage changes on the superconducting gravimeter of the geodetic observatory Wettzell, Germany. *Geophysics*, 73(6), WA95–WA104. <https://doi.org/10.1190/1.2992508>
- Dietermann, N., & Weiler, M. (2013). Spatial distribution of stable water isotopes in alpine snow cover. *Hydrology and Earth System Sciences*, 17(7), 2657–2668. <https://doi.org/10.5194/hess-17-2657-2013>
- Eaton, A. K., Rouse, W. R., Lafleur, P. M., Marsh, P., & Blanken, P. D. (2001). Surface energy balance of the Western and Central Canadian subarctic: Variations in the energy balance among five major terrain types. *Journal of Climate*, 14(17), 3692–3703. [https://doi.org/10.1175/1520-0442\(2001\)014<3692:Sebotw>2.0.Co;2](https://doi.org/10.1175/1520-0442(2001)014<3692:Sebotw>2.0.Co;2)
- Gat, J. R. (1996). Oxygen and hydrogen isotopes in the hydrologic cycle. *Annual Review of Earth and Planetary Sciences*, 24(1), 225–262. <https://doi.org/10.1146/annurev.earth.24.1.225>
- Glas, R., Lautz, L., McKenzie, J., Moucha, R., Chavez, D., Mark, B., & Lane, J. W. (2019). Hydrogeology of an alpine talus aquifer: Cordillera Blanca, Peru. *Hydrogeology Journal*, 27(6), 2137–2154. <https://doi.org/10.1007/s10040-019-01982-5>

- Gustafson, J. R., Brooks, P. D., Molotch, N. P., & Veatch, W. C. (2010). Estimating snow sublimation using natural chemical and isotopic tracers across a gradient of solar radiation. *Water Resources Research*, 46(12), W12511. <https://doi.org/10.1029/2009wr009060>
- Hayashi, M. (2020). Alpine hydrogeology: The critical role of groundwater in sourcing the headwaters of the world. *Groundwater*, 58, 498–510. <https://doi.org/10.1111/gwat.12965>
- Hood, J. L., & Hayashi, M. (2015). Characterization of snowmelt flux and groundwater storage in an alpine headwater basin. *Journal of Hydrology*, 521, 482–497. <https://doi.org/10.1016/j.jhydrol.2014.12.041>
- Hood, J. L., Roy, J. W., & Hayashi, M. (2006). Importance of groundwater in the water balance of an alpine headwater lake. *Geophysical Research Letters*, 33(13), 482–497. <https://doi.org/10.1029/2006gl026611>
- Huss, M., Farinotti, D., Bauder, A., & Funk, M. (2008). Modelling runoff from highly glacierized alpine drainage basins in a changing climate. *Hydrological Processes*, 22(19), 3888–3902. <https://doi.org/10.1002/hyp.7055>
- Huth, A. K., Leydecker, A., Sickman, J. O., & Bales, R. C. (2004). A two-component hydrograph separation for three high-elevation catchments in the Sierra Nevada, California. *Hydrological Processes*, 18(9), 1721–1733. <https://doi.org/10.1002/hyp.1414>
- Immerzeel, W. W., Lutz, A. F., Andrade, M., Bahl, A., Biemans, H., Bolch, T., ... Baillie, J. E. M. (2020). Importance and vulnerability of the world's water towers. *Nature*, 577(7790), 364–369. <https://doi.org/10.1038/s41586-019-1822-y>
- Jodar, J., Cabrera, J. A., Martos-Rosillo, S., Ruiz-Constan, A., Gonzalez-Ramon, A., Lamban, L. J., ... Custodio, E. (2017). Groundwater discharge in high-mountain watersheds: A valuable resource for downstream semi-arid zones. The case of the Berchules River in Sierra Nevada (southern Spain). *Sci Total Environ*, 593–594, 760–772. <https://doi.org/10.1016/j.scitotenv.2017.03.190>
- Jonas, T., Marty, C., & Magnusson, J. (2009). Estimating the snow water equivalent from snow depth measurements in the Swiss Alps. *Journal of Hydrology*, 378(1–2), 161–167.
- Juen, I., Kaser, G., & Georges, C. (2007). Modelling observed and future runoff from a glacierized tropical catchment (cordillera Blanca, Perú). *Global and Planetary Change*, 59(1), 37–48. <https://doi.org/10.1016/j.gloplacha.2006.11.038>
- Kimmeier, F., Bouzelboudjen, M., Ornstein, P., Weber, I., & Rouiller, J.-D. (2001). Geohydrological parameters identification and groundwater vulnerability to pollution: A Swiss case study. Paper presented at: 3rd international conference on future groundwater resources at risk, Lisbon, Portugal.
- Kudryavtsev, S. M. (2004). Improved harmonic development of the earth tide-generating potential. *Journal of Geodesy*, 77(12), 829–838. <https://doi.org/10.1007/s00190-003-0361-2>
- Langston, G., Bentley, L. R., Hayashi, M., McClymont, A., & Pidlisecky, A. (2011). Internal structure and hydrological functions of an alpine proglacial moraine. *Hydrological Processes*, 25, 2967–2982. <https://doi.org/10.1002/hyp.8144>
- Lehmann-Horn, J. A., Walbrecker, J. O., Hertrich, M., Langston, G., McClymont, A. F., & Green, A. G. (2011). Imaging groundwater beneath a rugged proglacial moraine. *Geophysics*, 76(5), B165–B172. <https://doi.org/10.1190/geo2011-0095.1>
- Leirião, S., He, X., Christiansen, L., Andersen, O. B., & Bauer-Gottwein, P. (2009). Calculation of the temporal gravity variation from spatially variable water storage change in soils and aquifers. *Journal of Hydrology*, 365(3), 302–309. <https://doi.org/10.1016/j.jhydrol.2008.11.040>
- Li, Y. C., & Sideris, M. G. (1994). Improved gravimetric terrain corrections. *Geophysical Journal International*, 119(3), 740–752. <https://doi.org/10.1111/j.1365-246X.1994.tb04013.x>
- Liu, F., Williams, M. W., & Caine, N. (2004). Source waters and flow paths in an alpine catchment, Colorado front range, United States. *Water Resources Research*, 40(9), W09401. <https://doi.org/10.1029/2004wr003076>
- Longman, I. M. (1959). Formulas for computing the tidal accelerations due to the moon and the sun. *Journal of Geophysical Research (1896–1977)*, 64(12), 2351–2355. <https://doi.org/10.1029/JZ064i012p02351>
- Lugon, R., & Delaloye, R. (2001). Modelling alpine permafrost distribution, Val de Rechy, Valais Alps (Switzerland). *Norsk Geografisk Tidsskrift - Norwegian Journal of Geography*, 55(4), 224–229. <https://doi.org/10.1080/00291950152746568>
- Marthaler, M., Sartori, M., Escher, A., & Meisser, N. (2008). Vissoie (Feuille 1307) - with explanatory text. Swisstopo, O.f.d.t. (ed), Federal Office of Topography swisstopo, Bern, Switzerland.
- McClymont, A. F., Hayashi, M., Bentley, L. R., & Liard, J. (2012). Locating and characterising groundwater storage areas within an alpine watershed using time-lapse gravity, GPR and seismic refraction methods. *Hydrological Processes*, 26(12), 1792–1804. <https://doi.org/10.1002/hyp.9316>
- McClymont, A. F., Hayashi, M., Bentley, L. R., Muir, D., & Ernst, E. (2010). Groundwater flow and storage within an alpine meadow-talus complex. *Hydrology and Earth System Sciences*, 14(6), 859–872. <https://doi.org/10.5194/hess-14-859-2010>
- McClymont, A. F., Roy, J. W., Hayashi, M., Bentley, L. R., Maurer, H., & Langston, G. (2011). Investigating groundwater flow paths within proglacial moraine using multiple geophysical methods. *Journal of Hydrology*, 399(1–2), 57–69. <https://doi.org/10.1016/j.jhydrol.2010.12.036>
- Moore, R. (2005). Introduction to salt dilution gauging for streamflow measurement: Part 3. *Streamline Watershed Management Bulletin*, 7(4), 20–23.
- Muir, D. L., Hayashi, M., & McClymont, A. F. (2011). Hydrological storage and transmission characteristics of an alpine talus. *Hydrological Processes*, 25, 2954–2966. <https://doi.org/10.1002/hyp.8060>
- Pauritsch, M., Wagner, T., Winkler, G., & Birk, S. (2016). Investigating groundwater flow components in an alpine relict rock glacier (Austria) using a numerical model. *Hydrogeology Journal*, 25(2), 371–383. <https://doi.org/10.1007/s10040-016-1484-x>
- Priestley, C. H. B., & Taylor, R. J. (1972). On the assessment of surface heat flux and evaporation using large-scale parameters. *Monthly Weather Review*, 100(2), 81–92. [https://doi.org/10.1175/1520-0493\(1972\)100<0081::AIDJCLI>2.0.CO;2](https://doi.org/10.1175/1520-0493(1972)100<0081::AIDJCLI>2.0.CO;2)
- Rau, G.C. (2019). PyGTide v0.2. Retrieved from <https://doi.org/10.5281/zenodo.1346664>
- Rohrer, M., Salzmann, N., Stoffel, M., & Kulkarni, A. V. (2013). Missing (in-situ) snow cover data hampers climate change and runoff studies in the greater Himalayas. *Science of the Total Environment*, 468–469(Suppl), S60–70. <https://doi.org/10.1016/j.scitotenv.2013.09.056>
- Roy, J. W., & Hayashi, M. (2009). Multiple, distinct groundwater flow systems of a single moraine–talus feature in an alpine watershed. *Journal of Hydrology*, 373(1–2), 139–150. <https://doi.org/10.1016/j.jhydrol.2009.04.018>
- Saunders, I. R., Bailey, W. G., & Bowers, J. D. (1997). Evaporation regimes and evaporation modelling in an alpine tundra environment. *Journal of Hydrology*, 195(1), 99–113. [https://doi.org/10.1016/S0022-1694\(96\)03242-8](https://doi.org/10.1016/S0022-1694(96)03242-8)
- Schaad, W. (1995). The origin of Rauhewackes (Cornieules) by the karstification of gypsum. *Ecologiae Geologicae Helveticae*, 88(1), 59–90.
- Schmieder, J., Hanzer, F., Marke, T., Garvelmann, J., Warscher, M., Kunstmann, H., & Strasser, U. (2016). The importance of snowmelt spatiotemporal variability for isotope-based hydrograph separation in a high-elevation catchment. *Hydrology and Earth System Sciences*, 20(12), 5015–5033. <https://doi.org/10.5194/hess-20-5015-2016>
- Scintrex Ltd. (2012). *CG-5 Scintrex Autograv system operation manual*. Concord, Canada: Scintrex Ltd.
- Somers, L. D., McKenzie, J. M., Mark, B. G., Lagos, P., Ng, G.-H. C., Wickert, A. D., ... Silva, Y. (2019). Groundwater buffers decreasing

- glacier melt in an Andean watershed—But not forever. *Geophysical Research Letters*, 46(22), 13016–13026. <https://doi.org/10.1029/2019gl084730>
- Stichler, W., Schotterer, U., Fröhlich, K., Ginot, P., Kull, C., Gäggeler, H., & Pouyaud, B. (2001). Influence of sublimation on stable isotope records recovered from high-altitude glaciers in the tropical Andes. *Journal of Geophysical Research: Atmospheres*, 106(D19), 22613–22620. <https://doi.org/10.1029/2001jd900179>
- SwissTopo (2020 and 2015). <https://map.geo.admin.ch>
- SwissTopo (2018) Geocover GA25 1:25'000 - Geological vector datasets for better subsurface management, Switzerland.
- Vincent, A., Violette, S., & Aðalgeirsdóttir, G. (2019). Groundwater in catchments headed by temperate glaciers: A review. *Earth-Science Reviews*, 188, 59–76. <https://doi.org/10.1016/j.earscirev.2018.10.017>
- Viviroli, D., Dürr, H. H., Messerli, B., Meybeck, M., & Weingartner, R. (2007). Mountains of the world, water towers for humanity: Typology, mapping, and global significance. *Water Resources Research*, 43(7), W07447. <https://doi.org/10.1029/2006wr005653>
- Wenzel, H.-G. (1996). The nanogal software: Earth tide data processing package ETERNA 3.30, bull. Inf. *Marées Terrestres*, 124, 9425–9439.

#### SUPPORTING INFORMATION

Additional supporting information may be found online in the Supporting Information section at the end of this article.

**How to cite this article:** Arnoux M, Halloran LJS, Berdat E, Hunkeler D. Characterizing seasonal groundwater storage in alpine catchments using time-lapse gravimetry, water stable isotopes and water balance methods. *Hydrological Processes*. 2020;34:4319–4333. <https://doi.org/10.1002/hyp.13884>